



OPEN

SUBJECT AREAS:

CELL BIOLOGY

BIOMARKERS

MOLECULAR BIOLOGY

BIOMARKER RESEARCH

Sex differences in skeletal muscle Phosphatase and tensin homolog deleted on chromosome 10 (PTEN) levels: A cross-sectional study

M. Constantine Samaan^{1,2}, Sonia S. Anand^{3,4,5,6}, Arya M. Sharma⁷, Imtiaz A. Samjoo^{1,5}
& Mark A. Tarnopolsky^{1,5}

Received

14 November 2014

Accepted

10 February 2015

Published

17 March 2015

Correspondence and requests for materials should be addressed to M.C.S. (samaanc@mcmaster.ca)

¹Department of Pediatrics, McMaster University, Hamilton, Ontario, Canada, ²Division of Pediatric Endocrinology, McMaster Children's Hospital, Hamilton, Ontario, Canada, ³Population Genomics Program, Chanchlani Research Centre, McMaster University, Hamilton, ON, Canada, ⁴Population Health Research Institute, Hamilton Health Sciences and McMaster University, Hamilton, Ontario, Canada, ⁵Department of Medicine, McMaster University, Hamilton, Ontario, Canada, ⁶Department of Clinical Epidemiology/Biostatistics, McMaster University, Hamilton, Ontario, Canada, ⁷University of Alberta, Edmonton, Alberta, Canada.

Women have higher adiposity but maintain insulin sensitivity when compared to men. Phosphatase and tensin homolog deleted on chromosome 10 (PTEN) inhibits insulin signaling, but it is not known if PTEN regulate insulin resistance in a sex-specific manner. In this cross-sectional study, muscle biopsies from participants in the Molecular Study of Health and Risk in Ethnic Groups (Mol-SHARE) were used to test for sex differences in PTEN expression. Quantitative real-time PCR was performed to determine PTEN gene expression (n = 53), and western blotting detected total and phosphorylated PTEN protein (n = 36). Study participants were comparable in age and body mass index. Women had higher fat mass percentage compared to men (40.25 ± 9.9% in women versus 27.6 ± 8.8% in men; mean difference -0.18, 95% CI (-0.24, -0.11), p-value <0.0001), with similar HOMA-IR (2.46 ± 2.05 in men versus 2.34 ± 3.06 in women; mean difference 0.04; 95% CI (-0.12, 0.21), p-value 0.59). Women had significant downregulation of PTEN gene expression (p-value 0.01) and upregulation of PTEN protein phosphorylation (inactivation) (p-value 0.001) when compared to men after correction for age, ethnicity, HOMA-IR, fat mass and sex. We conclude that the downregulation of muscle PTEN may explain the retention of insulin sensitivity with higher adiposity in women compared to men.

One of the main hallmarks of obesity is the deposition of excess fat in depots within and outside the adipose tissue¹, and the increased adiposity seen in obesity is associated with skeletal muscle insulin resistance². As skeletal muscle is the main organ responsible for postprandial glucose disposal³, its insulin resistance is a major contributor to the global epidemic of type 2 diabetes⁴⁻⁷. Understanding the mechanisms driving muscle insulin resistance is key to treating and preventing type 2 diabetes, as it will allow the implementation of specific interventions designed to restore insulin sensitivity.

One of the factors that determine adiposity patterns is sex. It is well known that women have a higher fat mass when compared to men⁸. Importantly, despite women having higher adiposity, this does not appear to adversely impact insulin sensitivity when compared to men at a given weight^{9,10}. This important observation may be explained by sex-based differential expression of molecules that regulate the insulin-signaling pathway.

One of the molecules that regulate muscle insulin signaling is Phosphatase and tensin homolog deleted on chromosome 10 (PTEN)^{11,12}. PTEN inhibits insulin-stimulated Phosphatidylinositol-3-kinase/Akt (PI3K/Akt) signaling, and is reported to be upregulated in muscle of obese mice¹³. It is not known whether sex differences in muscle PTEN expression contribute to equivalent insulin sensitivity despite higher adiposity in women when compared to men.

We hypothesized that lower muscle PTEN expression levels results in the relative retention of insulin sensitivity despite higher adiposity in women compared to men.



Table 1 | Clinical characteristics of the participants

Variable	Male (n = 42)		Female (34)		Mean Difference	95% Confidence Interval		P-value
	Mean	SD	Mean	SD		Lower	Upper	
Age (years)	34.64	10.22	34.76	10.68	0.0007	-0.06	0.07	0.98
Height (cm)	175.40	6.99	164.01	6.52	0.03	0.02	0.04	<0.0001
Weight (kg)	84.44	12.96	73.06	16.64	0.06	0.03	0.10	0.001
BMI (kg/m²)	27.26	3.98	27.35	6.32	0.004	-0.03	0.04	0.81
Waist circumference (cm)	96.24	12.51	88.36	12.70	0.036	0.01	0.07	0.02
Hip circumference (cm)	105.40	9.48	109.08	12.06	-0.014	-0.03	0.01	0.18
Heart rate (bpm)	64.79	11.68	65.68	7.47	-0.003	-0.04	0.03	0.86
Systolic BP (mmHg)	113.10	9.26	108.88	9.69	0.017	-0.001	0.04	0.07
Diastolic BP (mmHg)	74.38	9.15	72.68	6.53	0.005	-0.02	0.03	0.65
Fat mass (kg)	22.60	10.06	29.20	13.30	-0.31	-0.56	-0.05	0.02

bpm = beats per minute; BP = blood pressure.

Results

The study group included 34 women and 42 men, and gene expression data were available on 53 (n = 21 female) and protein data on 36 participants (n = 15 female). Men and women were of similar age and had similar body mass index (BMI) (Table 1).

Of note, four women were on oral contraceptive therapy, and one was on estrogen therapy.

Women have higher fat mass compared to men. When comparing body composition between women and men, women had significantly higher fat mass percentage, which was mainly due to higher superficial subcutaneous fat in comparison to men. On the other hand, men had higher lean mass and waist-to-hip ratio when compared to women (Table 2). There were no differences between men and women in HOMA-IR (2.46 ± 2.05 in men versus 2.34 ± 3.06 in women, mean difference 0.04; 95% CI (-0.12, 0.21)) (Table 3).

Muscle PTEN gene expression is lower in women compared to men. To test whether there are sex differences in muscle PTEN levels, we first analyzed PTEN gene expression levels in muscle using Quantitative Real-Time PCR (qRT-PCR). In the unadjusted analysis, PTEN gene expression was significantly lower in women when compared to men (Figure 1, p-value < 0.0001).

This lower muscle PTEN gene expression in women persisted after adjustment for age, ethnicity, fat mass percentage, and log HOMA-IR (Table 4, β -0.31; 95% CI (-0.54, -0.08), p-value 0.01).

Total muscle PTEN protein expression is similar in women & men. In order to determine if the reduction in gene expression in women is associated with reduced PTEN protein levels, we performed western blot analysis on muscle lysates from men and women.

PTEN gene expression did not correlate with PTEN protein levels in muscle (p-value 0.35). However, unadjusted normalized total PTEN protein levels (PTEN/GAPDH) were similar in men and

women (Figure 2, p-value 0.2), and this remained after adjustment for age, ethnicity, fat mass percentage, and log HOMA-IR (Table 4, β 0.39; 95% CI (-0.08, 0.87), p-value 0.1).

Women have higher muscle PTEN protein phosphorylation (inactivation) compared to men. To determine if there were differences in PTEN protein activity, we measured the phosphorylated (inactivated) version of PTEN protein. Women had higher pPTEN/PTEN ratio (Figure 3, unadjusted analysis p-value 0.002; Figure 4), and this persisted with adjustment for age, ethnicity, fat mass percentage, and log HOMA-IR (Table 4, β 0.85; 95% CI (0.38, 1.32), p-value 0.001). This higher pPTEN/PTEN ratio indicates the presence of more inactive PTEN protein in muscle of women when compared to men.

Discussion

At similar BMI levels, women maintain their insulin sensitivity when compared to men despite having higher adiposity⁹. In this study, we investigated the sex differences in muscle PTEN gene expression, protein content and activity to see if PTEN downregulation is involved in this paradox.

We demonstrate that women have lower muscle PTEN gene expression when compared to men, despite having higher adipose tissue mass. This is coupled with increased inactivation of PTEN protein.

PTEN is a dual protein and lipid phosphatase that interferes with the insulin-signaling pathway via its lipid phosphatase activity. PTEN itself can be inactivated by phosphorylation¹⁴⁻¹⁶, and this post-translational modification impact PTEN activity. PTEN can autoinhibit itself through S380-385 sites, whereby phosphorylation of S385 leads to the phosphorylation of S380 and Threonine sites, and binding of the COOH tail to the C2 and phosphatase domains, preventing the binding of PTEN to a complex of protein that drive its activity¹⁷.

Table 2 | Characteristics of the lean and fat mass compartments in men and women

Variable	Male (n = 42)		Female (34)		Mean Difference	95% Confidence Interval		P-value
	Mean	SD	Mean	SD		Lower	Upper	
% Fat mass	27.6	8.8	40.25	9.86	-0.18	-0.24	-0.11	<0.0001
WHR	0.91	0.08	0.81	0.07	0.05	0.03	0.07	<0.0001
Lean mass (kg)	57.6	7	40.5	4.3	0.15	0.13	0.17	<0.0001
SAT (cm²)	224.9	103	277.44	139.97	-0.1	-0.2	0.01	0.069
Superficial SAT (cm²) (n = 40 male, n = 28 female)	100.57	33.71	137.93	76.36	-0.12	-0.22	-0.02	0.006
Deep SAT (cm²) (n = 42 male, n = 31 female)	152.44	83.47	173.67	123.42	-0.02	-0.13	0.09	0.56
VAT (cm²)	126.51	75.32	105.77	65.58	0.07	-0.06	0.21	0.27

WHR = waist-to-hip ratio; SAT = subcutaneous adipose tissue; VAT = visceral adipose tissue.



Table 3 | Metabolic phenotype and PTEN gene and protein expression (n = 76 unless otherwise stated)

Variable	Male		Female		Mean Difference	95% Confidence Interval		P-value
	Mean	SD	Mean	SD		Lower	Upper	
FBG (mmol/l)	5.03	0.52	4.87	0.66	0.02	-0.01	0.04	0.18
Fasting insulin (μU/ml)	10.68	8.01	13.29	20.69	-0.003	-0.16	0.16	0.97
Cholesterol (mmol/l)	4.75	1.06	4.64	0.88	0.007	-0.04	0.05	0.73
Triglycerides (mmol/l)	1.51	1.09	1.12	0.69	0.01	-0.02	0.21	0.11
HDL (mmol/l)	1.23	0.33	1.44	0.33	-0.08	-0.13	-0.02	0.01
LDL (mmol/l)	2.89	0.94	2.66	0.67	0.02	-0.05	0.1	0.52
HOMA-IR	2.46	2.05	2.34	3.06	0.04	-0.12	0.21	0.59
Log PTEN gene expression (n = 53, SE)	0.13	0.07	-0.44	0.09	0.57	0.33	0.8	<0.0001
Log PTEN/GAPDH protein ratio (n = 36, SE)	-0.26	0.07	-0.12	0.09	-0.14	-0.37	0.08	0.20
Log pPTEN/PTEN protein ratio (n = 36, SE)	-0.27	0.05	-0.001	0.06	-0.27	-0.43	-0.11	0.002

SD = standard deviation; SE = standard error; FBG = fasting blood glucose; HDL = high-density lipoprotein; LDL = low-density lipoprotein; HOMA-IR = homeostatic model assessment-insulin resistance; GAPDH = glyceraldehyde 3-phosphate dehydrogenase.

In addition, Casein Kinase II (CK2) phosphorylates PTEN (S370, S385), but the biological importance of this is uncertain¹⁸. CK2 also seem to prime certain sites (S362, T366) for phosphorylation via the glycogen synthase kinase-3 β (GSK3 β) pathway. The latter sites form a feedback loop to inhibit growth factor signaling via the PI3K pathway and PTEN. Interestingly, neither CK2 nor GSK3 β affect S380 phosphorylation¹⁹.

In addition, RhoA-associated kinase (ROCK), acting on the C2 domain of PTEN, upregulate leukocyte chemotaxis via phosphorylation and activation of S229, T232, T319, and T321 sites²⁰. In contrast, PI3K p110 δ subunit inactivates PTEN in macrophages through inhibition of RhoA/ROCK²¹.

In addition, it has been shown that leptin plays an important role in phosphorylation (inhibition) of PTEN in the hypothalamus²², but the significance of this is uncertain.

The PTEN-mediated downregulation of insulin signaling may be explained by the presence of negative feedback loops in the insulin signaling pathway itself that become activated with increased adiposity, including Forkhead box O (FOXO) proteins and Mammalian

Target Of Rapamycin Complex 1 (mTORC1) and its downstream effector S6K 1 and 2^{23–26}.

In obese mice with normal ability to express PTEN, there is upregulation of muscle PTEN protein that is associated with reduced insulin signaling¹³. In addition, muscle-specific PTEN knockout mice have enhanced insulin sensitivity when rendered obese²⁷. In contrast, transgenic overexpression of PTEN in mice leads to hyperphagia yet lower adiposity. Interestingly, this is coupled with reduced insulin signaling but maintained insulin sensitivity. This maintenance of insulin sensitivity in transgenic mice is due to increased brown adipose tissue activity, which promotes energy expenditure and lowers nutrient storage^{28,29}.

In humans, polymorphisms of *PTEN* gene leading to higher PTEN expression levels have been noted in diabetes³⁰. In contrast, *PTEN* haploinsufficiency seen in Cowden syndrome, a cancer predisposition syndrome, is associated with obesity and paradoxical enhancement of insulin sensitivity³¹. Taken together, the above lines of evidence suggest that PTEN has direct and indirect effects on insulin sensitivity and signaling in different organs in rodents and humans.

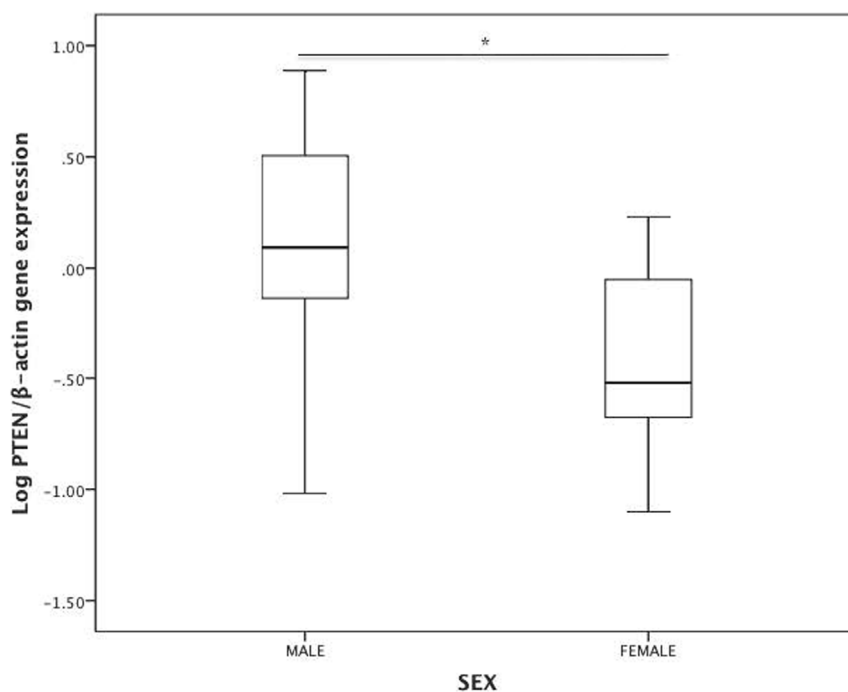
Figure 1 | Log PTEN/ β -actin (n = 53) gene expression in men and women.



Table 4 | The general linear model analysis of PTEN gene expression and PTEN/GAPDH and pPTEN/PTEN protein content in muscle

Gene expression data (Log PTEN/actin)				
Parameter	β	95% Confidence Interval		P-value
Age/years	-0.005	-0.02	0.01	0.36
Ethnicity	-0.13	-0.37	0.18	0.3
Log HOMA-IR	-0.15	-0.65	0.36	0.56
Log %FM	-0.58	-1.65	0.5	0.29
Sex	-0.43	-0.75	-0.11	0.01
Protein data (Log PTEN/GAPDH)				
Parameter	β	95% Confidence Interval		P-value
Age/years	0.003	-0.12	0.02	0.69
Ethnicity	-0.25	-0.49	-0.01	0.046
Log HOMA-IR	0.04	-0.4	0.48	0.85
Log %FM	-0.08	-0.94	0.78	0.85
Sex	0.24	-0.05	0.52	0.1
Protein data (Log pPTEN/PTEN)				
Parameter	β	95% Confidence Interval		P-value
Age/years	0.01	-0.01	0.02	0.27
Ethnicity	-0.08	-0.26	0.11	0.4
Log HOMA-IR	-0.15	-0.47	0.18	0.37
Log %FM	-0.48	-1.21	0.16	0.14
Sex	0.39	0.17	0.6	0.001

%FM = fat mass percentage.

In our study, the downregulation of PTEN gene expression and PTEN protein inactivation in women may protect against the inhibition of PI3K/Akt signaling with increased adiposity. As low levels of Akt activity are needed to maintain maximal glucose uptake²⁵, even relatively small reductions in PTEN activity can result in maintained insulin action despite higher adiposity levels in women when compared to men.

The sex differences in muscle insulin sensitivity may be explained by differences in sex steroids^{32,33}. Estrogen, mainly a female hormone, stimulates muscle Akt signaling and glucose transporter 4 gene expression independently of insulin^{32,33}. In addition, post-menopausal women have reduced insulin sensitivity that improves with estradiol therapy³⁴, and insulin resistance was noted in men with defects in estrogen synthesis or response^{35,36}. The mechanisms

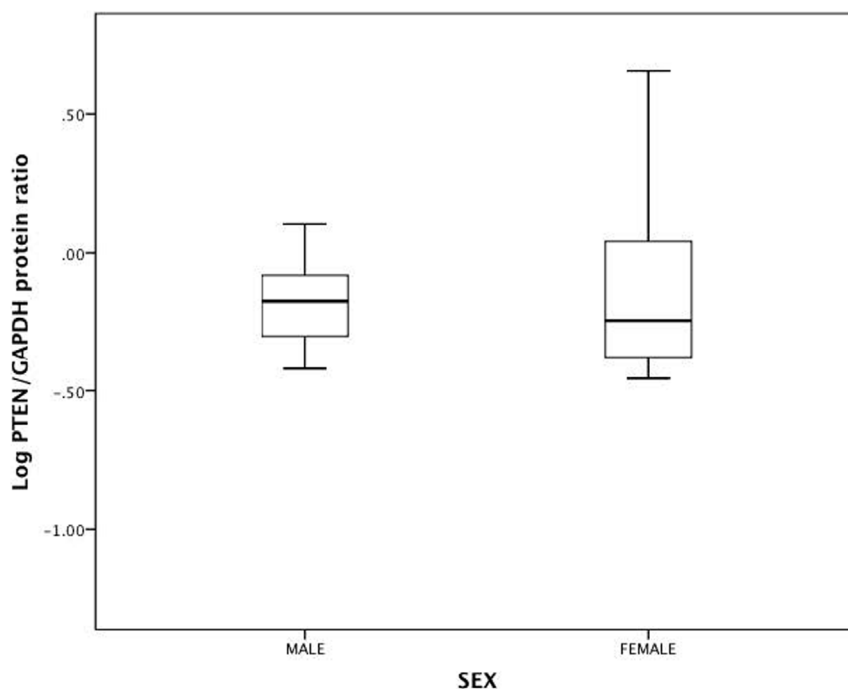


Figure 2 | Log PTEN/GAPDH protein ratio (n = 36) in men and women. GAPDH = glyceraldehyde 3-phosphate dehydrogenase.

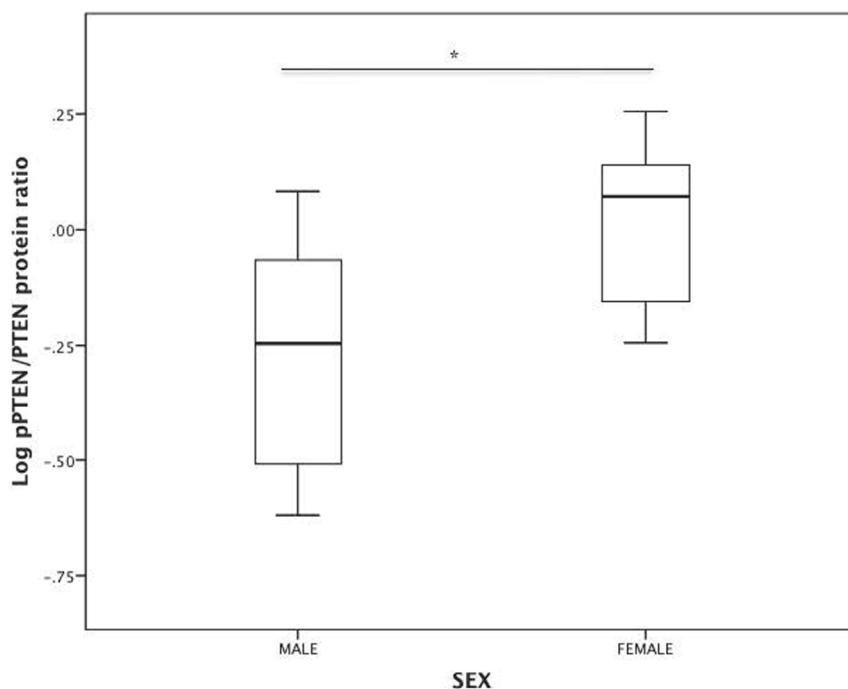


Figure 3 | Log pPTEN/PTEN protein ratio (n = 36) in men and women.

through which estrogen may interact with PTEN need to be clarified in future studies.

The strengths of this study include the relatively large sample size of muscle biopsies from well-characterized study participants, and the detailed characterization of PTEN at gene and protein expression levels.

We did not study the effects of insulin stimulation on PI3K/Akt pathway to correlate this with PTEN expression, as we did not treat the muscle tissue with insulin prior to freezing, which is a limitation of this study. In addition, we did not study adipose tissue insulin signaling or glucose uptake. In mice with adipose-specific PTEN deletion, increased adipose tissue insulin sensitivity was associated with reduced muscle insulin sensitivity, which may be an attempt to maintain whole body insulin sensitivity³⁷.

In summary, this study shows that muscle PTEN is regulated in a sex-specific manner, and makes PTEN an attractive therapeutic target in treatment and prevention of insulin resistance and type 2 diabetes.

Methods

The samples used in this report were from the Molecular Study of Health and Risk in Ethnic Groups (*Mol-SHARE study*). This study was designed to understand the mechanisms underlying ethnic variations in predisposition to adverse cardiometabolic outcomes, and compared South Asians to Europeans (ClinicalTrials.gov Identifier NCT00249314). The study recruited participants between 18–50 years of age, and study procedures and measurements have been reported previously³⁸. Total fat mass (FM) was measured using DXA scans after an overnight fast. Subcutaneous (SAT) and visceral adipose tissue (VAT) compartments were measured using MRI of the abdomen by attaining T1-weighted MRI image at the level of mid-L4 (TR 400 ms, TE 13 ms). The volume of SAT and VAT was determined by manual tracing of the specific fat depot.

The Hamilton Integrated Research Ethics Board approved the study, and all participants provided written informed consent. This study is utilizing a subset from the full study that has muscle biopsy samples available. The study was conducted in accordance with current clinical practice guidelines and legislation.

We used BMI cutoff points including 18.5–24.9 kg/m² for normal weight, 25–29.9 kg/m² for overweight, and ≥30 kg/m² to classify participants. In this analysis, we grouped subjects to maximize statistical power, and log-transformed values of HOMA-IR was used to provide a measure of insulin resistance.

Metabolic biomarkers. Study participants provided blood samples after an overnight fast (12 hours). Fasting serum lipid profile was generated using enzymatic methods for cholesterol³⁹, while serum LDL was calculated using the Friedewald formula⁴⁰, and

HDL was quantified with a homogenous enzymatic colorimetric assay (ROCHE/Hitachi Modular Package Insert). Glucose was measured using the hexokinase/glucose-6-phosphate dehydrogenase method⁴¹. Triglycerides were quantified with an enzymatic colorimetric assay (ROCHE/Hitachi Modular instrument and reagent kit). Insulin was quantified by an electrochemiluminescence immunoassay using the Roche Elecsys R 2010 immunoassay analyzer (Roche Diagnostics GmbH, Indianapolis, Indiana, USA). Insulin resistance was determined by calculating the homeostatic model assessment-insulin resistance (HOMA-IR)^{42,43}.

Muscle biopsy. Muscle biopsies were obtained from the vastus lateralis muscle under local anesthesia by a modified Bergstrom needle with suction³⁸.

Total RNA extraction. Trizol Reagent was purchased from Life Technologies and used in total RNA isolation. Muscle samples were homogenized in 1 ml Trizol with a power homogenizer on ice twice for 15 second interval at each attempt. The samples were mixed by inverting 4–5 times and placed at room temperature for 5 minutes. Then, 200 μ l chloroform was added, and samples were shaken vigorously for 15 seconds and left at room temperature for 2–3 minutes. The samples were then spun down at 12,000 g, 4°C, for 15 minutes. The aqueous phase was transferred to new tubes and 500 μ l isopropanol was added to the aqueous phase followed by a brief vortex. The samples were then left overnight at -20° C, and then centrifuged at 12,000 g, 4°C, for 15 minutes. The supernatant was decanted and 1 ml 70% ethanol added to the pellet and mixed with sample. Samples were then centrifuged at 7,500 g, 4°C, for 5 minutes. After air-drying the pellet, nuclease-free water was added to each tube and samples incubated at 55°C for 10 minutes. Samples were cooled down for 15 minutes at room temperature and RNA purity was measured with a spectrophotometer. RNA samples with 260/280 ratios at 1.8–2 were then used to synthesize cDNA.

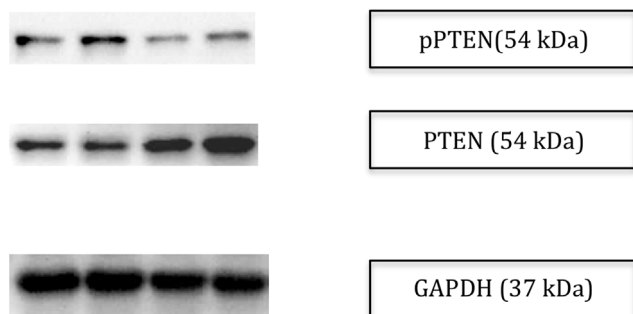
Reverse transcription reaction to generate cDNA. Reverse transcription reaction was performed using SuperScript[®] III First-Strand Synthesis kit (Invitrogen, Carlsbad, CA) following DNase treatment for 30 minutes at 37°C, and the reverse transcription reaction was conducted using 1 μ g of RNA as template according to the manufacturer's instructions.

Quantitative Real-Time PCR (qRT-PCR). PTEN gene expression analysis was conducted in triplicates using the Rotor-Gene 6000 qRT-PCR machine (Corbett Research; Mortlake, Australia). We used TaqMan[®] Gene Expression Assays (Applied Biosystems; Foster City, CA) of either PTEN (TaqMan assay Hs02621230_s1) or beta-Actin as the endogenous control gene (TaqMan assay Hs01060665_g1). Statistical analysis of qRT-PCR data was performed using the $\Delta\Delta$ Ct method⁴⁴.

Western blot. Quantification of PTEN and pPTEN muscle protein content was done using western blotting. Biopsies from vastus lateralis muscle were homogenized as previously described⁴⁵, and 50 μ g was loaded on an 8% polyacrylamide gel. Membranes were blocked in 5% BSA in TBST (0.1% Tween-20), and blots were incubated with PTEN, pPTEN^{Ser380} and GAPDH primary antibodies (Cell Signaling, dilution 1 : 1000) in 5% BSA in TBST. Anti-Rabbit IgG HRP-Linked (1 : 3000



Male



Female

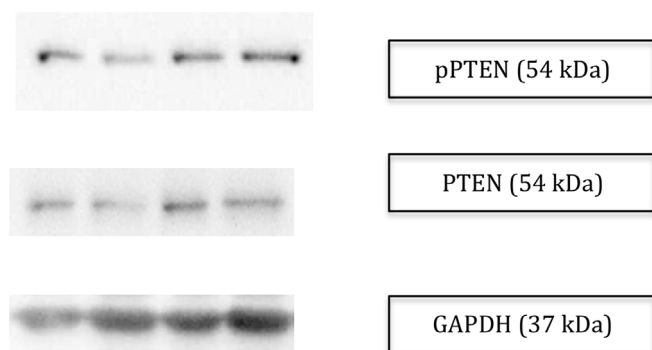


Figure 4 | Representative images for western blot data from (a) male and (b) female participants.

dilution) in 5% BSA in TBST was used as secondary antibody. Amersham™ ECL™ Western Blotting detection reagent (GE HealthCare) was used to detect the protein signal, and ImageJ software was used to quantify the protein density with normalization of PTEN to GAPDH and pPTEN^{Ser380} to total PTEN⁴⁶.

Statistical analysis. Data were tested for normality using Shapiro-Wilk test and log transformed if not normally distributed, and variance inflation factor was implemented to rule out collinearity. Independent sample t-test was used to compare the variables without adjustment, and two-tailed statistical significance results are reported. A general Linear Model was used in the analyses with PTEN gene expression, PTEN/GAPDH and PTEN/pPTEN as dependent variables and adjusting for age, fat mass percentage, HOMA-IR, ethnicity and sex as covariates. We report the mean differences between men and women and the respective 95% confidence intervals. Data are reported as mean ± SD unless otherwise stated, and significance was set at p-value of less than 0.05. SPSS version 22 was used for data analysis (Armonk, NY: IBM Corp).

- Gomez-Ambrosi, J. *et al.* Body mass index classification misses subjects with increased cardiometabolic risk factors related to elevated adiposity. *Int J Obes (Lond)* **36**, 286–294, doi:10.1038/ijo.2011.100 (2012).
- Kim, J. Y. *et al.* High-fat diet-induced muscle insulin resistance: relationship to visceral fat mass. *Am J Physiol Regul Integr Comp Physiol* **279**, R2057–2065 (2000).
- DeFronzo, R. A. & Tripathy, D. Skeletal Muscle Insulin Resistance Is the Primary Defect in Type 2 Diabetes. *Diabetes Care* **32**, S157–S163, doi:10.2337/dc09-S302 (2009).
- Martins, A. R. *et al.* Mechanisms underlying skeletal muscle insulin resistance induced by fatty acids: importance of the mitochondrial function. *Lipids Health Dis* **11**, 30, doi:10.1186/1476-511X-11-30 (2012).
- Kraegen, E. W., Cooney, G. J. & Turner, N. Muscle insulin resistance: a case of fat overconsumption, not mitochondrial dysfunction. *Proc Natl Acad Sci U S A* **105**, 7627–7628, doi:10.1073/pnas.0803901105 (2008).
- Danaei, G. *et al.* National, regional, and global trends in fasting plasma glucose and diabetes prevalence since 1980: systematic analysis of health examination surveys and epidemiological studies with 370 country-years and 2.7 million participants. *Lancet* **378**, 31–40, doi:10.1016/S0140-6736(11)60679-X (2011).
- Juarez-Lopez, C. *et al.* Insulin resistance and its association with the components of the metabolic syndrome among obese children and adolescents. *BMC public health* **10**, 318, doi:10.1186/1471-2458-10-318 (2010).
- Lemieux, S., Prud'homme, D., Bouchard, C., Tremblay, A. & Despres, J. P. Sex differences in the relation of visceral adipose tissue accumulation to total body fatness. *Am J Clin Nutr* **58**, 463–467 (1993).
- Faerch, K., Borch-Johnsen, K., Vaag, A., Jorgensen, T. & Witte, D. R. Sex differences in glucose levels: a consequence of physiology or methodological convenience? The Inter99 study. *Diabetologia* **53**, 858–865, doi:10.1007/s00125-010-1673-4 (2010).
- Geer, E. B. & Shen, W. Gender differences in insulin resistance, body composition, and energy balance. *Gender Medicine* **6**, Part 1, 60–75, doi:http://dx.doi.org/10.1016/j.genm.2009.02.002 (2009).
- Butler, M. *et al.* Specific Inhibition of PTEN Expression Reverses Hyperglycemia in Diabetic Mice. *Diabetes* **51**, 1028–1034, doi:10.2337/diabetes.51.4.1028 (2002).
- Lo, Y. T., Tsao, C. J., Liu, I. M., Liou, S. S. & Cheng, J. T. Increase of PTEN gene expression in insulin resistance. *Horm Metab Res* **36**, 662–666, doi:10.1055/s-2004-826016 (2004).
- Hu, Z. *et al.* PTEN Inhibition Improves Muscle Regeneration in Mice Fed a High-Fat Diet. *Diabetes* **59**, 1312–1320, doi:10.2337/db09-1155 (2010).
- Carracedo, A., Salmena, L. & Pandolfi, P. P. SnapShot: PTEN signaling pathways. *Cell* **133**, 550 e551 doi:10.1016/j.cell.2008.04.023 (2008).
- Samuels, Y. & Ericson, K. Oncogenic PI3K and its role in cancer. *Curr Opin Oncol* **18**, 77–82 (2006).
- Vanhaesebroeck, B., Guillermet-Guibert, J., Graupera, M. & Bilanges, B. The emerging mechanisms of isoform-specific PI3K signalling. *Nat Rev Mol Cell Biol* **11**, 329–341, doi:10.1038/nrm2882 (2010).
- Odriezola, L., Singh, G., Hoang, T. & Chan, A. M. Regulation of PTEN activity by its carboxyl-terminal autoinhibitory domain. *J Biol Chem* **282**, 23306–23315, doi:10.1074/jbc.M611240200 (2007).
- Miller, S. J., Lou, D. Y., Seldin, D. C., Lane, W. S. & Neel, B. G. Direct identification of PTEN phosphorylation sites. *FEBS Lett* **528**, 145–153 (2002).
- Al-Khouri, A. M., Ma, Y., Togo, S. H., Williams, S. & Mustelin, T. Cooperative phosphorylation of the tumor suppressor phosphatase and tensin homologue (PTEN) by casein kinases and glycogen synthase kinase 3beta. *J Biol Chem* **280**, 35195–35202, doi:10.1074/jbc.M503045200 (2005).
- Li, Z. *et al.* Regulation of PTEN by Rho small GTPases. *Nature cell biology* **7**, 399–404, doi:10.1038/ncb1236 (2005).
- Papakonstanti, E. A., Ridley, A. J. & Vanhaesebroeck, B. The p110delta isoform of PI 3-kinase negatively controls RhoA and PTEN. *EMBO J* **26**, 3050–3061, doi:10.1038/sj.emboj.7601763 (2007).
- Ning, K. *et al.* A novel leptin signalling pathway via PTEN inhibition in hypothalamic cell lines and pancreatic beta-cells. *EMBO J* **25**, 2377–2387, doi:10.1038/sj.emboj.7601118 (2006).
- Carracedo, A. & Pandolfi, P. P. The PTEN-PI3K pathway: of feedbacks and cross-talks. *Oncogene* **27**, 5527–5541, doi:10.1038/onc.2008.247 (2008).
- Hoehn, K. L. *et al.* Insulin resistance is a cellular antioxidant defense mechanism. *Proc Natl Acad Sci U S A* **106**, 17787–17792, doi:10.1073/pnas.0902380106 (2009).
- Hoehn, K. L. *et al.* IRS1-independent defects define major nodes of insulin resistance. *Cell Metab* **7**, 421–433, doi:10.1016/j.cmet.2008.04.005 (2008).
- Hay, N. Interplay between FOXO, TOR, and Akt. *Biochim Biophys Acta* **1813**, 1965–1970, doi:10.1016/j.bbamcr.2011.03.013 (2011).
- Wijesekara, N. *et al.* Muscle-specific Pten deletion protects against insulin resistance and diabetes. *Mol Cell Biol* **25**, 1135–1145, doi:10.1128/MCB.25.3.1135-1145.2005 (2005).
- Ortega-Molina, A. *et al.* Pten positively regulates brown adipose function, energy expenditure, and longevity. *Cell Metab* **15**, 382–394, doi:10.1016/j.cmet.2012.02.001 (2012).
- Garcia-Cao, I. *et al.* Systemic elevation of PTEN induces a tumor-suppressive metabolic state. *Cell* **149**, 49–62, doi:10.1016/j.cell.2012.02.030 (2012).
- Ishihara, H. *et al.* Association of the polymorphisms in the 5'-untranslated region of PTEN gene with type 2 diabetes in a Japanese population. *FEBS Lett* **554**, 450–454 (2003).
- Pal, A. *et al.* PTEN mutations as a cause of constitutive insulin sensitivity and obesity. *N Engl J Med* **367**, 1002–1011, doi:10.1056/NEJMoa1113966 (2012).
- Dieli-Conwright, C. M., Spektor, T. M., Rice, J. C. & Todd Schroeder, E. Oestrogen and SERM treatments influence oestrogen receptor coregulator gene expression in human skeletal muscle cells. *Acta Physiol (Oxf)* **197**, 187–196, doi:10.1111/j.1748-1716.2009.01997.x (2009).
- Rogers, N. H., Witzczak, C. A., Hirshman, M. F., Goodyear, L. J. & Greenberg, A. S. Estradiol stimulates Akt, AMP-activated protein kinase (AMPK) and TBC1D1/4, but not glucose uptake in rat soleus. *Biochem Biophys Res Commun* **382**, 646–650, doi:10.1016/j.bbrc.2009.02.154 (2009).
- D'Eon, T. M. *et al.* Estrogen regulation of adiposity and fuel partitioning. Evidence of genomic and non-genomic regulation of lipogenic and oxidative pathways. *J Biol Chem* **280**, 35983–35991, doi:10.1074/jbc.M507339200 (2005).
- Herrmann, B. L., Janssen, O. E., Hahn, S., Broecker-Preuss, M. & Mann, K. Effects of estrogen replacement therapy on bone and glucose metabolism in a male with congenital aromatase deficiency. *Horm Metab Res* **37**, 178–183, doi:10.1055/s-2005-861292 (2005).



36. Smith, E. P. *et al.* Estrogen resistance caused by a mutation in the estrogen-receptor gene in a man. *N Engl J Med* **331**, 1056–1061, doi:10.1056/NEJM199410203311604 (1994).
37. Kurlawalla-Martinez, C. *et al.* Insulin hypersensitivity and resistance to streptozotocin-induced diabetes in mice lacking PTEN in adipose tissue. *Mol Cell Biol* **25**, 2498–2510, doi:10.1128/MCB.25.6.2498-2510.2005 (2005).
38. Anand, S. S. *et al.* Adipocyte hypertrophy, fatty liver and metabolic risk factors in South Asians: the Molecular Study of Health and Risk in Ethnic Groups (mol-SHARE). *PLoS One* **6**, e22112, doi:10.1371/journal.pone.0022112 (2011).
39. Allain, C. C., Poon, L. S., Chan, C. S., Richmond, W. & Fu, P. C. Enzymatic determination of total serum cholesterol. *Clin Chem* **20**, 470–475 (1974).
40. Friedewald, W. T., Levy, R. I. & Fredrickson, D. S. Estimation of the concentration of low-density lipoprotein cholesterol in plasma, without use of the preparative ultracentrifuge. *Clin Chem* **18**, 499–502 (1972).
41. Neeley, W. E. Simple automated determination of serum or plasma glucose by a hexokinase-glucose-6-phosphate dehydrogenase method. *Clin Chem* **18**, 509–515 (1972).
42. Matthews, D. R. *et al.* Homeostasis model assessment: insulin resistance and beta-cell function from fasting plasma glucose and insulin concentrations in man. *Diabetologia* **28**, 412–419 (1985).
43. Wallace, T. M., Levy, J. C. & Matthews, D. R. Use and Abuse of HOMA Modeling. *Diabetes Care* **27**, 1487–1495, doi:10.2337/diacare.27.6.1487 (2004).
44. Livak, K. J. & Schmittgen, T. D. Analysis of relative gene expression data using real-time quantitative PCR and the 2^{-Delta Delta C(T)} Method. *Methods* **25**, 402–408, doi:10.1006/meth.2001.1262 (2001).
45. Safdar, A. *et al.* Endurance exercise rescues progeroid aging and induces systemic mitochondrial rejuvenation in mtDNA mutator mice. *Proceedings of the National Academy of Sciences* **108**, 4135–4140, doi:10.1073/pnas.1019581108 (2011).
46. Schneider, C. A., Rasband, W. S. & Eliceiri, K. W. NIH Image to ImageJ: 25 years of image analysis. *Nat Meth* **9**, 671–675, doi:doi:10.1038/nmeth.2089 (2012).

Acknowledgments

We would like to acknowledge the participants in the study. We also thank Dr. Mohammed Khan (M.K.) for laboratory technical assistance. M.C.S. is supported by the New Investigator Fund Grant from Hamilton Health Sciences (Grant no. NIF-11272). Mol-SHARE study is funded by Heart & Stroke Foundation of Ontario, Canada (Project#: NA5702)

Author contributions

M.C.S., M.A.T. and S.S.A. conceived the study hypothesis. M.C.S., M.A.T., S.S.A., A.M.S. and I.A.S. conceived and designed the experiments. M.C.S., M.K. and I.A.S. performed experimental work. M.C.S., M.A.T., S.S.A. and I.A.S. analyzed the data and M.C.S. wrote the first draft, and all authors provided feedback to the submitted version of the manuscript.

Additional information

Competing financial interests: The authors declare no competing financial interests.

How to cite this article: Samaan, M.C., Anand, S.S., Sharma, A.M., Samjoo, I.A. & Tarnopolsky, M.A. Sex differences in skeletal muscle Phosphatase and tensin homolog deleted on chromosome 10 (PTEN) levels: A cross-sectional study. *Sci. Rep.* **5**, 9154; DOI:10.1038/srep09154 (2015).



This work is licensed under a Creative Commons Attribution 4.0 International License. The images or other third party material in this article are included in the article's Creative Commons license, unless indicated otherwise in the credit line; if the material is not included under the Creative Commons license, users will need to obtain permission from the license holder in order to reproduce the material. To view a copy of this license, visit <http://creativecommons.org/licenses/by/4.0/>